PHILOSOPHICAL TRANSACTIONS B

rstb.royalsocietypublishing.org

Research

Cite this article: Jimenez JC, Barichivich J, Mattar C, Takahashi K, Santamaría-Artigas A, Sobrino JA, Malhi Y. 2018 Spatio-temporal patterns of thermal anomalies and drought over tropical forests driven by recent extreme climatic anomalies. *Phil. Trans. R. Soc. B* **373**: 20170300.
http://dx.doi.org/10.1098/rstb.2017.0300

Accepted: 23 August 2018

One contribution of 22 to a discussion meeting issue 'The impact of the 2015/2016 El Niño on the terrestrial tropical carbon cycle: patterns, mechanisms and implications'.

Subject Areas:
environmental science, ecology

Keywords:
warming, drought, tropical forests, scPDSI, El Niño

Author for correspondence:
Juan C. Jimenez
e-mail: jcjm@uv.es

Electronic supplementary material is available online at https://dx.doi.org/10.6084/m9.figshare.c.4218065.

THE ROYAL SOCIETY PUBLISHING

Spatio-temporal patterns of thermal anomalies and drought over tropical forests driven by recent extreme climatic anomalies

Juan C. Jimenez[1], Jonathan Barichivich[2,3,4], Cristian Mattar[5], Ken Takahashi[6], Andrés Santamaría-Artigas[7,8], José A. Sobrino[1] and Yadvinder Malhi[9]

[1]GCU/IPL, University of Valencia, Catedratico Jose Beltran 2, 46980 Paterna, Valencia, Spain
[2]Instituto de Conservación, Biodiversidad y Territorio, Facultad de Ciencias Forestales y Recursos Naturales, Universidad Austral de Chile, Casilla 567, Valdivia, Chile
[3]Center for Climate and Resilience Research, Blanco Encalada 2002, piso 4, Santiago, Chile
[4]Instituto de Geografía, Pontificia Universidad Católica de Valparaíso, Avenida Brasil N° 2241 Valparaíso, Chile. CP 2362807
[5]Universidad de Aysén, Coyhaique, Chile, CP 5950000
[6]SENHAMI, Jr. Cahuide 785, 15072, Lima, Peru
[7]Department of Geographical Sciences, University of Maryland, College Park, MD 20742, USA
[8]NASA Goddard Space Flight Center (GSFC) Terrestrial Information Systems Laboratory Code 619, Greenbelt, MD, USA
[9]Environmental Change Institute, Oxford University Centre for the Environment, South Parks Road, Oxford OX1 3QY, UK

JCJ, 0000-0001-7562-4895; YM, 0000-0002-3503-4783

The recent 2015–2016 El Niño (EN) event was considered as strong as the EN in 1997–1998. Given such magnitude, it was expected to result in extreme warming and moisture anomalies in tropical areas. Here we characterize the spatial patterns of temperature anomalies and drought over tropical forests, including tropical South America (Amazonia), Africa and Asia/Indonesia during the 2015–2016 EN event. These spatial patterns of warming and drought are compared with those observed in previous strong EN events (1982–1983 and 1997–1998) and other moderate to strong EN events (e.g. 2004–2005 and 2009–2010). The link between the spatial patterns of drought and sea surface temperature anomalies in the central and eastern Pacific is also explored. We show that indeed the EN2015–2016 led to unprecedented warming compared to the other EN events over Amazonia, Africa and Indonesia, as a consequence of the background global warming trend. Anomalous accumulated extreme drought area over Amazonia was found during EN2015–2016, but this value may be closer to extreme drought area extents in the other two EN events in 1982–1983 and 1997–1998. Over Africa, datasets disagree, and it is difficult to conclude which EN event led to the highest accumulated extreme drought area. Our results show that the highest values of accumulated drought area over Africa were obtained in 2015–2016 and 1997–1998, with a long-term drying trend not observed over the other tropical regions. Over Indonesia, all datasets suggest that EN 1982–1983 and EN 1997–1998 (or even the drought of 2005) led to a higher extreme drought area than EN2015–2016. Uncertainties in precipitation datasets hinder consistent estimates of drought severity over tropical regions, and improved reanalysis products and station records are required.

This article is part of a discussion meeting issue 'The impact of the 2015/2016 El Niño on the terrestrial tropical carbon cycle: patterns, mechanisms and implications'.

1. Introduction

El Niño-Southern Oscillation (ENSO) is the main cause of interannual variability in the atmospheric carbon dioxide growth rate anomalies even when the seasonal cycle and the long-term upward trend are removed [1]. Some studies

suggest that the atmospheric concentration of CO_2 increases during El Niño (EN) events, with the tropical forests playing a crucial role because they become a net source of carbon to the atmosphere [2]. This also occurs during severe drought events not necessarily linked to an EN event [3]. Other factors such as deforestation, degradation and disturbance have been key in driving tropical forests to act as a net carbon source during this past decade [4].

In recent years, research has focused mainly on the most extensive tropical rainforest region in Amazonia, where severe droughts have occurred with a frequency of 5 years: 2005, 2010 and 2015. Long-term monitoring through forest censuses suggests a weakening of the Amazon carbon sink [5] and a particular sensitivity to drought [6]. Recent research has also pointed out a decline of forest resilience to wildfires because of an intensification of the interactions between extreme droughts and fire [7,8]. In general, recent severe droughts over Amazonia were linked to warm sea surface temperature (SST) anomalies over the tropical Pacific (EN) and over the tropical Atlantic [9–12], producing a decrease in rainfall, low river water levels, high risk of forest fire and impacts on natural river ecosystems [13]. Although most studies focused on the Pacific and Atlantic forcing of Amazonian climate variability, there is evidence that anomalies in vegetation greenness are linked to global interannual variations in SST, land surface temperature and precipitation worldwide [14], thus having an impact not only over Amazonia but also over African and Asian forests. Recent research suggests an intensification of the dry season over most African forests, with the drying associated with enhanced sea surface warming over the Indian Ocean and warming in the tropical North Atlantic (TNA) [15,16]. In the case of Asian forests, the ENSO and the Indian Ocean dipole (IOD) play a key role on regional climate variability because of their modulation of the monsoon system [17].

The recent 2015–2016 EN occurred in a decade of rapid warming background, and consequently, it ranked among the three strongest EN events in recent decades [18]. This EN event led to record-breaking temperature anomalies and precipitation deficits over some tropical regions [19], with still uncertain implications for the carbon balance of the tropical forests and global atmospheric CO_2 concentrations [20]. A large carbon source during late 2015 was observed over the tropics [21], with the three major tropical regions of South America, Africa and Asia releasing similar amounts of carbon to the atmosphere but due to different carbon exchange processes [22]. This EN event coincided with anomalously high temperatures over the Indian Ocean, and with moderate warming over the TNA.

This paper aims to analyse the spatial and temporal patterns of thermal anomalies and drought over tropical forests during EN2015–2016 in the context of the previous strong EN events and also in the context of long-term variations. The datasets and methods used in this study are described in §2. Section 3 discusses the warming and drought patterns observed during EN2015–2016, and §4 discusses the warming and drought patterns observed during EN1982–1983 and EN1997–1998, as well as during the moderate EN2004–2005 and EN2009–2010. This section also includes an analysis of the long-term time series of temperature and drought. In §5, we briefly discuss the link between central Pacific (CP) and eastern Pacific (EP) SST anomalies and the observed pattern of drought over land. Section 6 presents our concluding remarks.

2. Datasets and methods

(a) Delimitation of the study area

The spatial and temporal patterns of warming and drought analysed in this paper are for the major tropical forest regions. The study area for tropical forests was selected using moderate resolution imaging spectroradiometer (MODIS) Land Cover product (MCD12C1) and pixels classified as 'Evergreen Broadleaf Forests (EBF)' within the 30 N–30 S latitude band. The spatial resolution of the Land Cover product (0.05°) was aggregated to 0.5° for comparison with the spatial resolution of climate datasets. Only aggregated pixels with a percentage of EBF high-resolution pixels (0.05°) higher than 75% were selected for analysis (electronic supplementary material, figure S1). The selected area includes mainly rainforests in South America (Amazon Basin), Africa (Democratic Republic of Congo, Gabon, Congo, Cameroon, Central African Republic, Equatorial Guinea) and Asia (mainly Indonesia, including Borneo, Sumatra and New Guinea/Papua New Guinea). For simplicity, we will refer to these study areas as Amazonia, Africa and Asia or Indonesia. The term pantropical will be used to refer to the whole tropical forest area.

(b) Temperature and drought data

We used monthly air (2 m) temperatures from European Center for Medium-Range Weather Forecasts (ECMWF) ECMWF Re-Analysis (ERA) Interim reanalysis [23] 'Monthly Means of Daily Means' (MMDM) product (0.75° × 0.75° resolution). A recent study found a broad agreement between temperature datasets, and ERA-Interim was also found to be a robust dataset for the analysis of temperatures in 2015 and 2016 and for long-term trend assessments [24]. Thermal anomalies were categorized into 'moderate', 'severe' and 'extreme' based on the values of standardized air temperature anomalies (*z*-score), which can be easily interpreted in terms of significance level (*p*-value). These three warming levels were assigned to the standardized anomalies ranges of 1.65–1.96 (moderate), 1.96–2.58 (severe) and greater than 2.58 (extreme), with *p*-values of 0.10–0.05, 0.05–0.01 and less than 0.01, respectively.

We analysed time series and spatial patterns of monthly, seasonal (JFM, AMJ, JAS and OND) and yearly anomalies, including also standardized anomalies. In some particular cases, we also considered half-yearly anomalies (JFMAMJ, JASOND or AMJJAS). The reference period (climatological mean) used to compute the anomalies was 1981–2010. Standardized anomalies were calculated as the ratio of the anomaly and the standard deviation of the climatological mean. All products were resampled to a common grid of 0.5°. It is worth mentioning that we analysed actual anomalies, so the background global warming trend was not removed from the temporal series. Results from linear trend removal will be commented on in §6 and electronic supplementary material, figures.

Drought variability was characterized using the self-calibrating Palmer drought severity index (scPDSI) [25], which allows the quantification of root-zone drought severity and extent using readily available monthly historical meteorological observations or reanalysis [20,26,27]. A basic soil moisture budget for the rooting zone is used to estimate the standardized moisture anomalies accounting for local soil water holding capacity, precipitation (moisture supply) and actual and potential evapotranspiration (PET; moisture demand). The only meteorological fields required for input are monthly

precipitation and PET. Since precipitation estimates over the tropics based on a single data stream are uncertain [27], we used the Multi-Source Weighted-Ensemble Precipitation (MSWEP) dataset [28] to calculate the scPDSI at a $0.5^\circ \times 0.5^\circ$ resolution from 1979 to 2016. Unlike other commonly used precipitation datasets, MSWEP combines the advantages of reanalysis, satellite and *in situ* records. Monthly PET was computed from wind, humidity and surface net radiation from the ERA-Interim reanalysis using the Penmann–Monteith formulation [20]. Soil water holding capacity data were extracted from the Food and Agriculture Organization digital soil map of the world [29]. The calibration of the index was done over the reference period 1979–2016. Moderate, severe and extreme drought severity levels were assigned to scPDSI ranges of −2 to −3, −3 to −4 and below −4, respectively.

Accumulated warmed area and drought area was also used as an indicator for the comparison between different EN events. Area affected by the different levels of standardized thermal anomalies and drought was extracted on a monthly basis, and then monthly areas were summed to obtain the accumulated area within a year. Accumulated area was expressed as percentage over the total area of the different tropical regions.

(c) Oceanic indices

The Oceanic El Niño Index (ONI) was used to characterize the strength of the recent EN event compared to other previous EN events. This index is calculated from the three month running mean of SST anomalies in the Niño 3.4 region (http://origin.cpc.ncep.noaa.gov/products/analysis_monitoring/ensostuff/ONI_v5.php). EN flavour was characterized through the E and C indices that correspond to SST anomaly patterns representing eastern and central equatorial Pacific warming, respectively. These two uncorrelated indices are based on the leading empirical orthogonal functions of tropical Pacific SST anomalies [30]. E and C indices were extracted from the Instituto Geofísico del Perú (IGP, www.met.igp.gob.pe/datos/EC.txt) (electronic supplementary material, figure S2). Oceanic indices for characterization of TNA and the IOD were also used. In this last case, the intensity of the IOD was represented by the gradient between western and south eastern equatorial Indian Ocean, named as Dipole Mode Index (DMI). These indices are also based on SST anomalies over specific oceanic regions. Values were extracted from 'The state of the ocean climate' initiative (http://sateteoftheocean.osmc.noaa.gov) (electronic supplementary material, figure S3).

3. Thermal anomalies and drought during EN 2015–2016

EN2015–2016 started developing by mid-2015, reaching its maximum intensity in late 2015 and early 2016 and to vanish by mid-2016. However, relatively high SST anomalies were also observed during mid- to late 2014. Figure 1 summarizes the state of the climate over tropical forests in terms of temperature and drought during this period. Figure 1*a* shows half-yearly standardized air temperature anomalies for the period 2014–2016 using the European reanalysis dataset ERA-interim. An incipient warming is observed at pantropical level in the second half of the year 2014, and warming was increasing during 2015 and early 2016. Although the intensity of warming was reduced in late 2016, it was still higher than the warming observed in late 2014 and early 2015. Therefore, warming over tropical forests remained in late 2016 when EN conditions had already vanished.

Monthly air temperature anomalies over the individual tropical regions for the years 2014, 2015 and 2016 are shown in figure 1*c*. Amazonia had positive temperature anomalies from 2014 to 2016, with maximum values from late 2015 to early 2016. Anomalies are mostly positive in the case of Africa and Asia, but the magnitude of the anomalies is lower than in Amazonia. Temperature anomalies were similar over all the three regions in 2014 and were typically below 0.5 K.

Figure 1*b* shows the spatial patterns of drought as represented by the scPDSI for the first and second half of 2014, 2015 and 2016. The first half of 2014 was characterized by a widespread wet pattern over Amazonia, whereas a dry pattern began to emerge over northeastern Amazonia during the second half of the year. This dry pattern spread over the rest of Amazonia during 2015 and 2016. However, the spatial pattern in 2015 is characterized by a wet–dry dipole from southwestern to northeastern Amazonia. This wet–dry dipole was maintained to some extent in 2016. The scPDSI indicated widespread and persistent dry conditions over African forests during the whole period between 2014 and 2016. Widespread dry conditions were also evident over Indonesia but only in the second half of 2015, though permanent dry conditions were observed over northern Borneo (Malaysia).

The temporal evolution of drought conditions over the three study areas is shown in figure 1*d*. In the case of the Amazon forests, a transition from widespread wet conditions in 2014 to intense dry conditions in 2016 is observed, whereas African forests remained under dry conditions over the whole period. Asian tropical forests experienced weaker drought conditions, with slightly negative values of scPDSI in 2014, a transition to dry conditions in 2015 and a recovery to neutral conditions in 2016.

4. EN 2015–2016 in the context of previous EN events

(a) EN events 1982–1983 and 1997–1998

The recent EN event rivals the other two strong EN events in 1982 and 1997, so it is informative to compare the spatial and temporal patterns of warming and drought to address similarities and differences between EN events (figure 2). Spatial patterns of standardized air temperature anomalies for the second half of 1982 and first half of 1983, and for the second half of 1997 and the first half of 1998, are illustrated in figure 2*a*. This figure can be compared to figure 1*a* to analyse the warming patterns for the three recent strong EN events 1982–1983, 1997–1998 and 2015–2016. EN1982–1983 was characterized by a widespread warming over Amazonia in the first half 1983, with almost neutral conditions in the second half of 1982. By contrast, during EN1997–1998 widespread heat anomalies over Amazonia are observed both in late 1997 and early 1998. These results also apply to African and Asian forests, although the magnitude of warming was weaker compared to Amazonia. Figure 2*c* shows that warming was only evident in early and mid-1983, whereas warming was observed from mid-1997 to almost the end of 1998. According to this warming feature, EN2015–2016 is more similar to EN1997–1998 than EN1982–1983 (figure 1*c*).

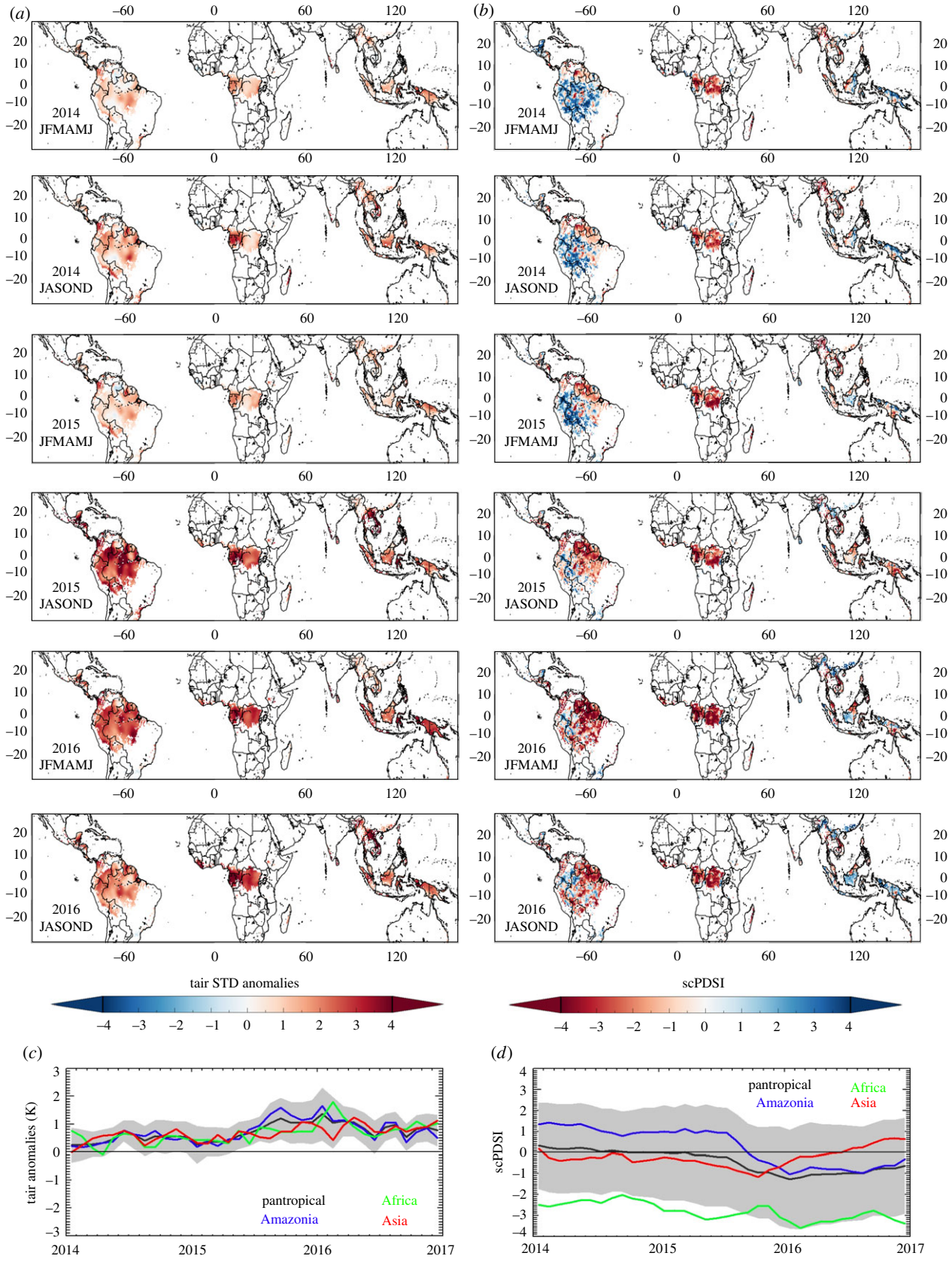

Figure 1. Spatial patterns of half-yearly (JFMAMJ and JASOND) (*a*) standardized air temperature anomalies and (*b*) drought index scPDSI, and mean monthly (*c*) air temperature anomalies and (*d*) scPDSI at pantropical level, over Amazonia, over Africa and over Asia for the period 2014–2016. Temperature anomalies were calculated from the ERA-interim product, and the scPDSI was calculated from the MSWEP precipitation dataset. Grey shading indicates the mean value at pantropical level within the $\pm 1\sigma$ interval.

The EN events 1982–1983 and 1997–1998 were characterized by widespread drought over Amazonia and Asia (figure 2*b*). In contrast, a widespread wet pattern was observed over Africa in 1982–1983 (except for some areas in the west of central Africa), and widespread drought was observed in 1997–1998. Moreover, spatially averaged values of scPDSI were negative over Amazonia and Asia during the whole period between 1981 and 1983, but almost neutral during 1996 and then negative during 1997 and 1998 (figure 2*d*). Moist conditions (greater than +1) prevailed

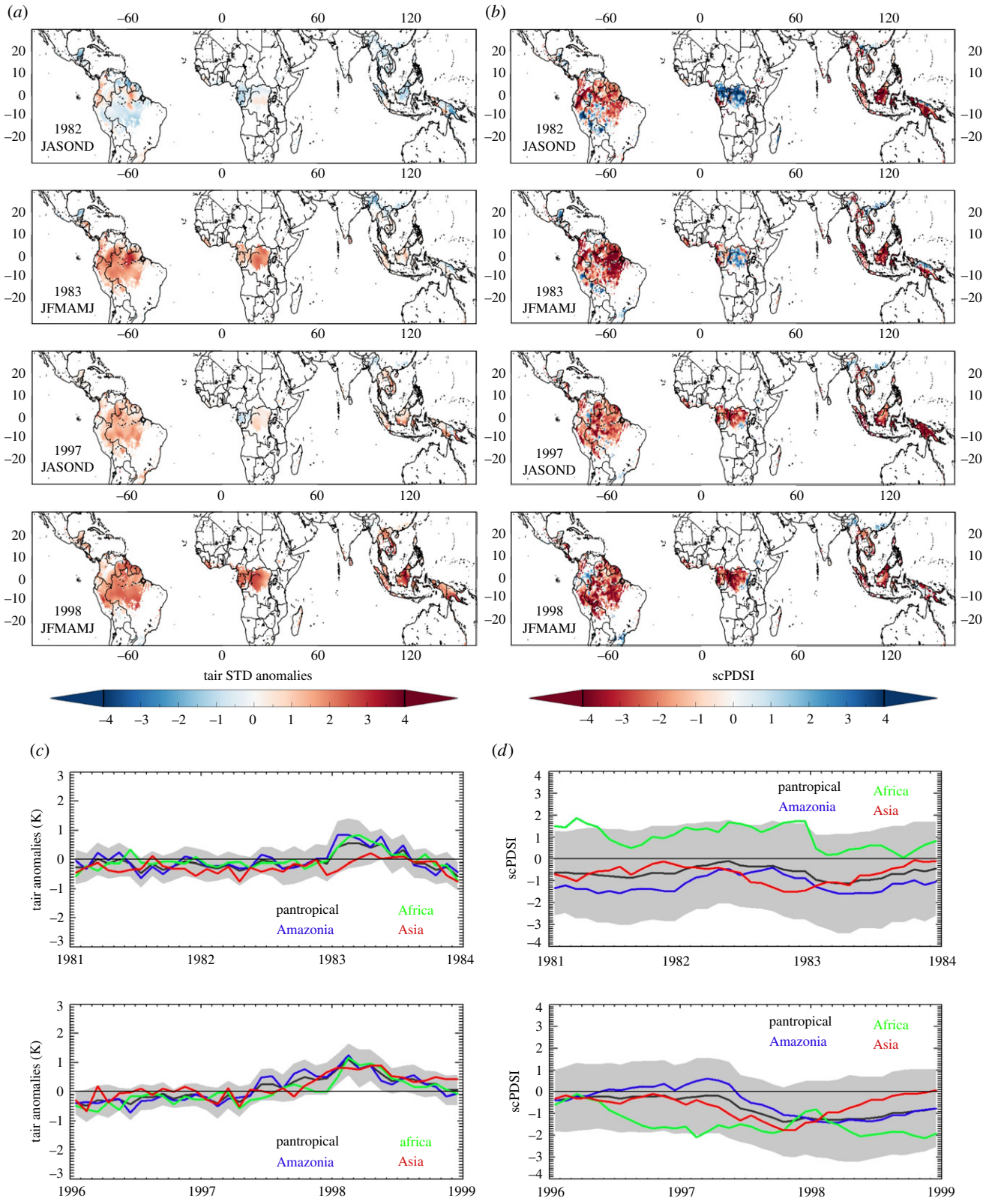

Figure 2. Spatial patterns of half-yearly (JFMAMJ and JASOND) (*a*) standardized air temperature anomalies and (*b*) scPDSI, and mean monthly (*c*) air temperature anomalies and (*d*) scPDSI at pantropical level, over Amazonia, over Africa and over Asia for the periods 1981–1983 and 1996–1998. Temperature anomalies were calculated from the ERA-interim product, and the scPDSI was calculated from the MSWEP precipitation dataset. Grey shading indicates the mean value at pantropical level within the $\pm 1\sigma$ interval.

over Africa during 1981 and 1982, and dry but close to neutral conditions during 1983.

(b) EN events in 2005 and 2010

Two severe drought events in 2005 and 2010 were widely reported over Amazonia. These droughts were attributed to anomalous high SSTs over the TNA, though 2004–2005 and especially 2009–2010 were also moderate EN events [9,11]. In contrast to EN events when effects usually peak during the boreal winter, the droughts of 2005 and 2010 peaked during the dry season (approximately from April to September). Six-month (AMJJAS) standardized air temperature anomalies show a stronger heat anomaly in 2005 over Amazonia and

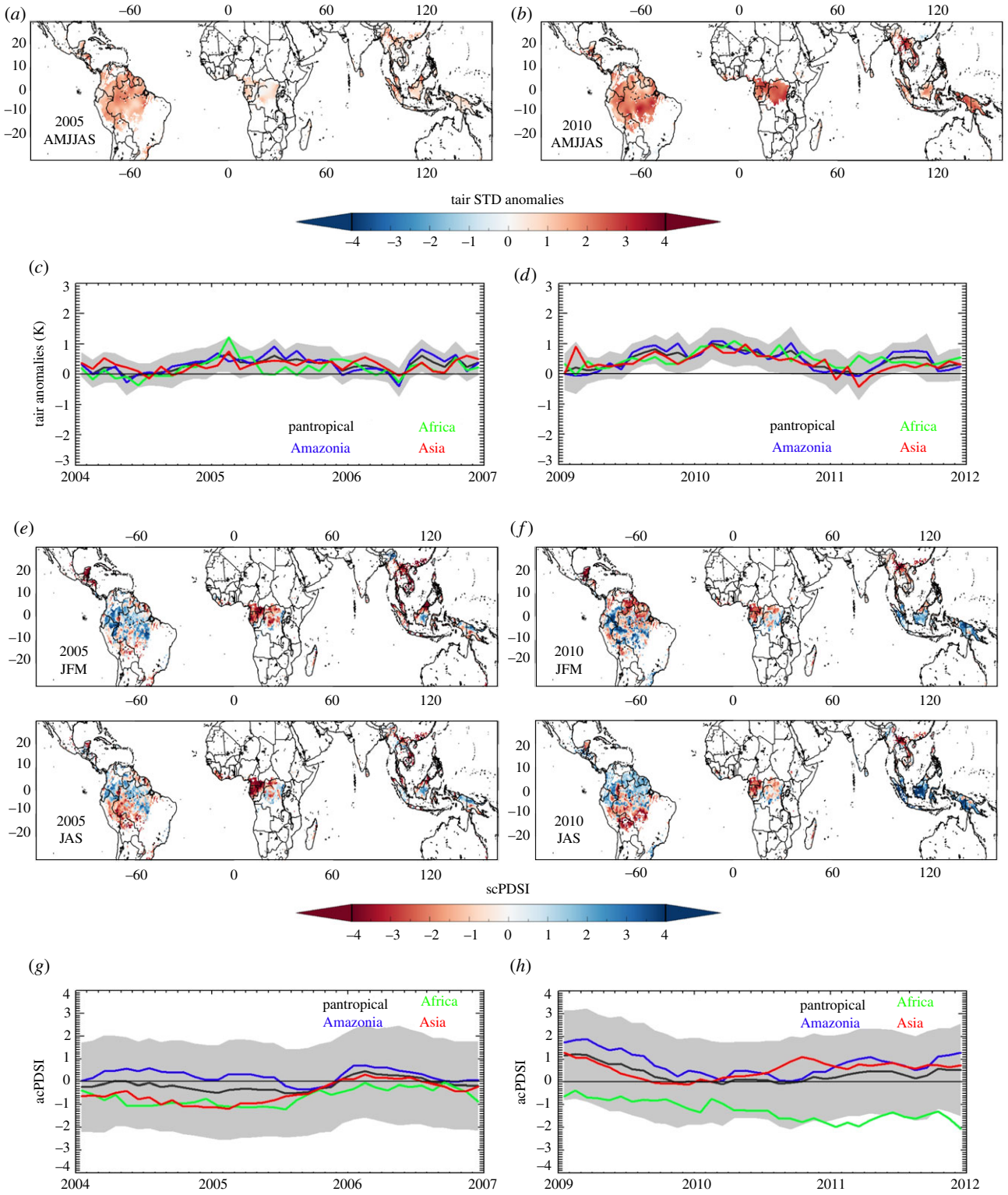

Figure 3. Spatial patterns of six-month (AMJJAS) standardized air temperature anomalies in (*a*) 2005 and (*b*) 2010, and mean monthly air temperature anomalies at pantropical level, and over Amazonia, over Africa, and over Asia for the periods (*c*) 2004–2005 and (*d*) 2009–2010. Spatial patterns of scPDSI for seasons JFM and JAS in (*e*) 2005 and (*f*) 2010, and mean monthly scPDSI at pantropical level, and over Amazonia, over Africa and over Asia for the periods (*g*) 2004–2005 and (*h*) 2009–2010. Temperature anomalies were calculated from the ERA-interim product, and the scPDSI was calculated from the MSWEP precipitation dataset. Grey shading indicates the mean value at pantropical level within the $\pm 1\sigma$ interval.

Africa compared to 2010 (figure 3*a*,*b*), with similar warming patterns over Asia in both years. However, because of the combination between EN followed by anomalous SSTs over TNA with a stronger EN event in 2009–2010 than in 2004–2005, the detailed seasonal evolution of temperature anomalies suggests that warming during the 2005 episode was mostly concentrated during the dry season from April to September, whereas the 2010 episode actually lasted from mid-2009 to mid-2010, with a weaker warming observed in JAS season in 2010 (results not shown).

Widespread warm anomalies were also observed over African forests in JAS-2005, and to lesser extent over some regions of Indonesia. Neutral conditions or weak warm anomalies were observed during 2009–2010 over Africa, with widespread warm anomalies over Asia in AMJ-2010. The highest values of monthly air temperature anomalies for the period

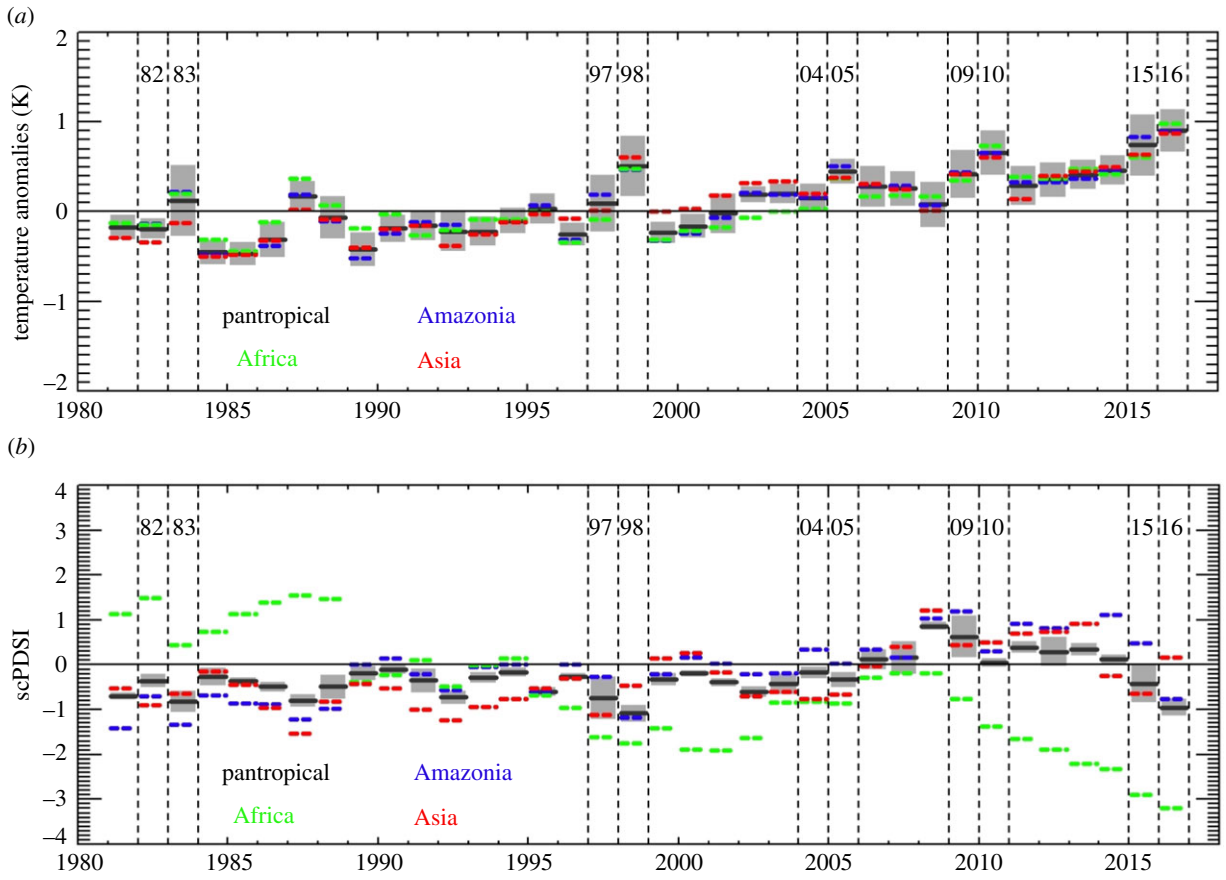

Figure 4. Time series of (*a*) yearly air temperature anomalies and (*b*) yearly scPDSI at pantropical level, and over Amazonia, over Africa and over Asia for the period 1981–2016. Temperature anomalies were calculated from the ERA-interim product, and the scPDSI was calculated from the MSWEP precipitation dataset. Grey shading indicates the mean value at pantropical level within the $\pm 1\sigma$ interval.

2004–2006 are systematically obtained over Africa, whereas monthly evolution for the period 2009–2011 is similar over the three regions, with the highest values observed over Amazonia along 2010 (figure 3*c*,*d*).

The spatial patterns of drought during the dry season (JAS) in 2005 and 2010 were similar over Amazonia, and were characterized by a north–south transition from wet to dry conditions (figure 3*e*,*f*). However, early 2005 is dominated by widespread wetness, whereas early 2010 shows a wet–dry dipole similar to that observed in the recent EN2015–2016 (figure 1*b*). We will discuss this similarity in §5. Dry conditions were also observed over African forests in 2005 and 2010, although the intensity of drought was higher over west Central Africa. Overall, Asia showed dry conditions in 2005 (especially in the early part of the year) and wet conditions in 2010. It is worth mentioning that widespread drought was not observed in monthly scPDSI at pantropical level and averaged over the Amazonian region because the mean scPDSI masks the dipole pattern and wet–dry values cancel out (mean scPDSI is close to zero and mostly positive during the periods 2004–2006 and 2009–2011 at pantropical level and over Amazonia; figure 3*g*,*h*). By contrast, the scPDSI averaged over the African forests area remained negative during 2004–2006 and 2009–2011.

(c) The long-term context

Results presented in previous sections allowed a comparison between temperature and drought patterns during EN2015–2016 and patterns over other strong/moderate EN events. However, other weak or moderate EN events occurred during these past decades (see ONI in electronic supplementary material, figure S2), added to other droughts as part of the interannual variability. Therefore, we show in this section the temporal evolution of temperature anomalies and drought during the period 1981–2016 to place the different events in a long-term context.

Figure 4 shows time series of yearly means for air temperature anomalies and the drought index scPDSI over the different tropical regions. Temperature anomalies (figure 4*a*) clearly evidence the peaks linked to strong EN events, with years 1998, 2010 and 2016 providing the highest temperature anomalies. A positive trend in temperature in line with the global warming trend, especially from year 2000, is also observed.

Droughts also peaked during strong EN events (figure 4*b*), but in contrast to air temperature anomalies the drought index shows significant differences between tropical regions, and a clear trend is not observed. The results obtained over tropical Africa are striking, with scPDSI values very different from the other regions. Africa was characterized by wet conditions in the 1980s, neutral conditions (except for the dry conditions observed during EN1997–1998) in the 1990s, and a kind of drying trend in the past decade (2005–2016).

Monthly temporal evolution of warming and drought severity over the different tropical forest regions is detailed in electronic supplementary material, figure S4. Some drought episodes had strong warming and drought severity over particular months concentrated on short time-periods, whereas other episodes led to a lower level of warming and severity but extended over a longer time-period. In order to take these two factors into account (warming/drought severity and duration), we show in figure 5 the accumulated area along one year for the period 1981–2016. The highest values of accumulated warmed area

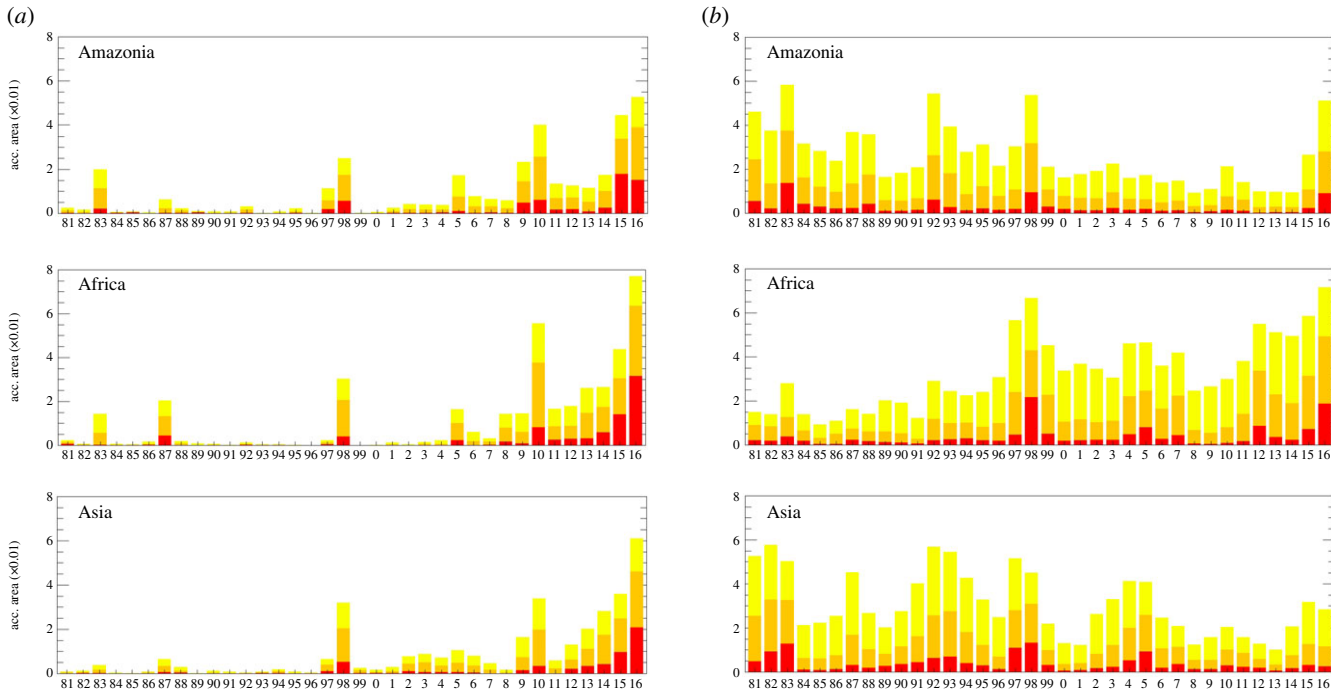

Figure 5. Time series of accumulated area affected by levels of (*a*) warm air temperature anomalies and (*b*) drought over Amazonia, over Africa and over Asia for the period 1981–2016. Moderate, severe and extreme levels are indicated by colour bars in yellow, orange and red, respectively.

(figure 5*a*) were obtained during EN2015–2016 in all the three regions, followed by EN2009–2010 and EN1997–1998, except in the case of Asia where EN2009–2010 provided a lower accumulated area than EN1997–1998. In terms of warming over Amazonia during the droughts in 2005 and 2010, the affected area was higher in 2010 than in 2005. Figure 5*a* also evidences an increasing long-term trend in warmed area, with a rapid increase from the 2000s.

In terms of drought area (figure 5*b*), Amazonia had a similar accumulated drought area during the three strong EN events (1982–1983, 1997–1998, 2015–2016), whereas over Africa the highest values of accumulated drought area were observed during EN2015–2016, closely followed by EN1997–1998. The episode of 2005 led also to significant accumulated area over African forests. Asia shows a progressive decrease in accumulated drought area during EN1982–1983, EN1997–1998, 2005 and 2010, with an increase during EN2015–2016. However, drought area over Asia during EN2015–2016 was lower than in 2005 and the other EN events. A clear trend is not observed in the accumulated area, but figure 5*b* suggests a decreasing trend over Amazonia, an increasing trend over Africa and neutral to decreasing trend over Asia (at least for the moderate levels of drought severity).

Spatial patterns of long-term trends in air temperature and precipitation (electronic supplementary material, figure S5) evidence a statistically significant warming trend over the three tropical regions for the JFM and JAS seasons. A wetting trend over most parts of Amazonia and a drying trend over tropical Africa (mainly over the west part of central Africa) are evidenced for the JFM season. However, a wetting trend is observed over Africa for the JAS season.

5. The role of ENSO flavours and other ocean regions

EN events in 1982–1983, 1997–1998 and 2015–2016 were the three strongest events since 1980, with similar ONI values (electronic supplementary material, figure S2). However, the different contribution of EP and CP anomalies are clearly evidenced through the E and C indices. The highest values of E index are found for EN1982–1983 and 1997–1998, whereas the highest value of C index is found for EN2015–2016, with a similar value to the C index for EN2009–2010 (electronic supplementary material, figure S2).

In general, anomalous convective heating during EN leads to generalized tropical tropospheric warming through equatorial atmospheric waves [31], which then communicates to the surface via energy fluxes [32]. Precipitation anomalies depend on the circulation changes, which depend more subtly on the convective heating patterns, so EP and CP EN can have different regional rainfall impacts [33]. These differences are evidenced in the similar wet/dry pattern in early 2016 and early 2010 over Amazonia (figures 1*b* and 3*f*) in contrast to drought patterns observed in other events.

In this section, we analysed the correlation between these indices and the scPDSI to evaluate whether this characteristic drought spatial pattern can be attributed to a particular ENSO flavour. CP and EP SST indices resulted in similar patterns of scPDSI variability (figure 6*a* and 6*b*, respectively), generally consistent with the typical ENSO precipitation patterns [34], but there are some regional differences. In Indonesia and New Guinea, drier conditions are stronger with warming in the CP than with warming in the EP [35], consistent with the more local control of SST on precipitation distribution. In northern South America, CP warming also leads to a stronger drying than the EP, with a particularly strong signal in eastern Amazon in boreal winter [20,33]. Conversely, EP warming has a local wet effect in western South America in boreal winter/spring associated with the southward displacement of the EP Intertropical Convergence Zone (ITCZ) [33,36,37] and a hint of the wet signal of EN in southeastern South America. In Africa, the signal associated with the individual C and E indices is not substantial, although there are hints of the wet signal in eastern equatorial Africa associated with CP warming in AMJ.

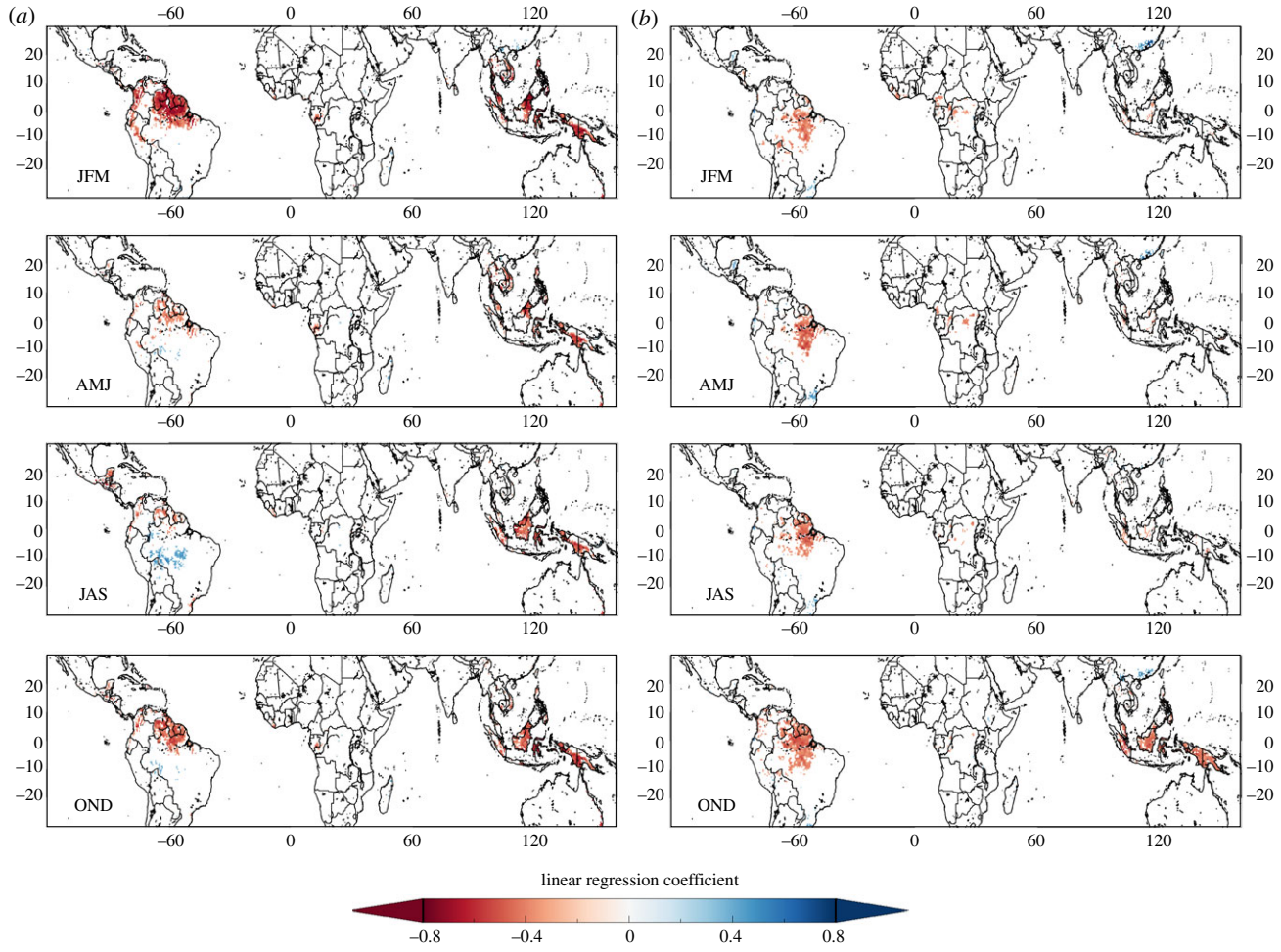

Figure 6. Linear correlation coefficient between scPDSI and (*a*) C index and (*b*) E index for the four seasons JFM, AMJ, JAS and OND. Only pixels with a statistical significance at $p < 0.05$ are displayed.

On the other hand, the 2015/2016 EN was an unusually strong event due to its high ratio between SST anomalies in the CP relative to the EP [18], which is consistent with its strong dry signal in northern South America (figure 1*b*) [20], but the wet anomaly in the western Amazon and the dry signal in western/central equatorial Africa observed during that event cannot be explained by the EN SST pattern. In contrast, this wet anomaly over Amazonia and dry anomaly over tropical Africa is driven by TNA SST anomalies, especially in JAS and OND seasons (electronic supplementary material, figure S6), leading also to a widespread wet signal over Asia. Overall, the effect of the Indian Ocean is weaker than tropical Pacific and Atlantic oceans, and impacts are focused on Asia (electronic supplementary material, figure S6). Positive DMI values induce a wet signal over Asia in the JFM season, but dryness in the OND season. Significant correlation is also observed during JFM over western Amazon (wet signal) and some regions of tropical Africa (dry signal).

6. Discussion and conclusion

We analysed temperature anomalies and the severity of drought over tropical forests during the course of EN event in 2015–2016 using different temperature and precipitation datasets. We also compared the 2015–2016 patterns with previous severe drought episodes linked to strong EN events (1982–1983, 1997–1998) and/or linked to EN events combined with SST anomalies in the tropical Atlantic (2005, 2010). Warming and drought over Amazonia were more severe in 2015–2016 than in the other recent droughts driven by Atlantic warming in 2005 and 2010. Warming in 2015–2016 was also stronger than that observed in the other EN events in 1982–1983 and 1997–1998, and it lasted longer (positive yearly mean temperature anomalies at basin level were only observed in 1983 during the course of EN1982–1983, and in 1997 and 1998 during EN1997–1998, but yearly means were positive in 2014, 2015 and 2016). There is also some evidence for a higher area extent affected by extreme drought in 2015–2016 when compared to previous drought episodes. Although this result should be taken with caution because of the differences between datasets, it is supported by other recent studies [8,38,39].

Previous studies also identified major drought conditions over Amazonia in 1988–1989, 1992, 2000 and 2006 [40]. We also identified these and other drought periods in the long-term analysis presented in §4c. These droughts are placed in the context of interannual variability, but they also occurred under other weaker EN events (see ONI in electronic supplementary material, figure S2). Furthermore, drought patterns in Amazonia are correlated with SST anomalies in different regions. In general, north–south drought patterns are linked to SST anomalies in the TNA and east–west patterns are observed during EN events [40,41]. However, different EN events can lead to varying drought patterns over Amazonia [42]. We found a similar east–west drought pattern during EN2009–2010 and 2015–2016, both characterized by a strong

SST anomaly over the Central Tropical Pacific (high C index value). This is also consistent with historic drought conditions found in Brazil during EN2009–2010 [43]. A linear correlation analysis showed that the dry pole over northern/northeastern Amazon is driven by SST anomalies in the EN region (with a stronger signal in the CP), but the wet pole over western/southwestern Amazon is not explained by anomalies in the EN region alone. In contrast, this wet pole seems to be driven by TNA anomalies and to lesser extent by the DMI.

Unlike Amazonia, it is believed that African forests are experiencing a long-term drying trend with occasional drought episodes [44]. The highest values of thermal anomalies and accumulated warmed area over Africa were also observed in 2015–2016, followed by the events in 1997–1998 and 2009–2010. Extreme drought was observed in 2015–2016, with similar accumulated area extents to those observed during EN1997–1998. It is worth mentioning that severe and extreme drought was also observed in the period 2004–2006, in agreement with high water deficits reported in 2005 by other studies (that continued in 2006 and 2007) [44]. Over tropical Africa, the link between drought and ENSO was not substantial, and dryness was driven mostly by anomalies in the TNA, with a weak signal attributed to the IOD, as also suggested by Malhi & Wright [45].

Asian forests experienced the strongest warming in 2005–2016 compared with the other events, but this was not translated into more severe drought. Drought severity was higher in 1982–1983, 1997–1998 and 2004–2005 than in 2015–2016. Similar to the African forests, a long-term drying trend has also been reported over Borneo, leading to progressive tree mortality and massive wildfires intensified during EN years [46]. We also found a different contribution of CP and EP SST anomalies, consistent with the influence of the two different types of EN on drought conditions over monsoon Asia, with decadal-scale drought attributed to CP EN events [17].

Overall, our results suggest that unprecedented warming was observed over tropical forests during the course of EN2015–2016 under a global warming trend. Unprecedented severe and extreme drought conditions were observed over some tropical regions, but similar or lower drought severity than other EN events was observed over other tropical regions. A previous study [20] showed that the magnitude of heat anomalies and drought during EN2015–2016 was enhanced by background increasing temperatures, at least over Amazonia. When warming trend is removed, the strength of EN2015–2016 may be reduced but still comparable to EN1997–1998 (electronic supplementary material, figure S7). We also found an increase in PET and vapour pressure deficit in 2015, which contributed to the drought patterns observed during EN2015–2016 (electronic supplementary material, figure S8).

Because different precipitation datasets may lead to distinct drought patterns over the tropics, especially over Africa [47], uncertainties in precipitation datasets are still an important limitation for drought severity assessment over these regions.

Data accessibility. Datasets used in this manuscript are available through the official web pages of the different providers. Datasets with a dedicated processing such as temperature anomalies and scPDSI, are available under request to the authors.

Authors' contributions. J.C.J., J.B. and C.M. conceived the study and carried out the data analysis. J.C.J. wrote the first draft of the paper. A.S.-A. contributed to the processing and information extraction from the reanalysis datasets. K.T. contributed to the analysis of the role of EN flavours. J.A.S. and Y.M. contributed to overall scientific discussion.

Competing interests. We have no competing interests.

Funding. J.B. acknowledges support from CONICYT/FONDAP/1511000.

Acknowledgements. We thank Francesca Di Giuseppe (ECMWF) for discussion on the performance of the ERA-interim precipitation product over tropical regions.

References

1. Jones CD, Collins M, Cox PM, Spall SA. 2001 The carbon cycle response to ENSO: a coupled climate-carbon cycle model study. *J. Clim.* **14**, 4113–4129. (doi:10.1175/1520-0442(2001)014,4113:TCCRTE>2.0.CO;2)
2. Cox PM, Pearson D, Booth BB, Friedlingstein P, Huntingford C, Jones CD, Luke CM. 2013 Sensitivity of tropical carbon to climate change constrained by carbon dioxide variability. *Nature* **494**, 341–344. (doi:10.1038/nature11882)
3. Gatti LV *et al.* 2014 Drought sensitivity of Amazonian carbon balance revealed by atmospheric measurements. *Nature* **506**, 76–80. (doi:10.1038/nature12957)
4. Baccini A, Walker W, Carvalho L, Farina M, Sulla-Menashe D, Houghton RA. 2017 Tropical forests are a net carbon source based on aboveground measurements of gain and loss. *Science* **358**, 230–234. (doi:10.1126/science.aam5962)
5. Brienen RJW *et al.* 2015 Long-term decline of the Amazon carbon sink. *Nature* **519**, 344–348. (doi:10.1038/nature14283)
6. Phillips OL *et al.* 2009 Drought sensitivity of the Amazon rainforest. *Science* **323**, 1344–1347. (doi:10.1126/science.1164033)
7. Brando PM *et al.* 2014 Abrupt increases in Amazonian tree mortality due to drought–fire interactions. *Proc. Natl. Acad. Sci. USA* **111**, 14 685–14 690. (doi:10.1073/pnas.1305499111)
8. Aragao LEOC *et al.* 2018 21st Century drought-related fires counteract the decline of Amazon deforestation carbon emissions. *Nat. Commun.* **9**, 536. (doi:10.1038/s41467-017-02771-y)
9. Marengo JA, Nobre CA, Tomasella J, Oyama MD, Sampaio de Oliveira G, De Oliveira R, Camargo H, Alves LM, Brown IF. 2008 The drought of Amazonia in 2005. *J. Clim.* **21**, 495–516. (doi:10.1175/2007JCLI1600.1)
10. Yoon JH, Zheng N. 2010 An Atlantic influence on Amazon rainfall. *Clim. Dyn.* **34**, 249–264. (doi:10.1007/s00382-009-0551-6)
11. Lewis SL, Brando PM, Phillips OL, van der Heijden GMF, Nepstad D. 2011 The 2010 Amazon drought. *Science* **331**, 554. (doi:10.1126/science.1200807)
12. Jiménez-Muñoz JC, Sobrino JA, Mattar C, Malhi Y. 2013 Spatial and temporal patterns of the recent warming of the Amazon forest. *J. Geophys. Res.* **118**, 5204–5215. (doi:10.1002/jgrd.50456)
13. Harris PP, Huntingford C, Cox PM. 2008 Amazon Basin climate under global warming: the role of the sea surface temperature. *Phil. Trans. R. Soc. B* **363**, 1753–1759. (doi:10.1098/rstb.2007.0037)
14. Los SO, Collatz GJ, Bounoua L, Sellers PJ, Tucker CJ. 2001 Global interannual variations in sea surface temperature and land surface vegetation, air temperature and precipitations. *J. Clim.* **14**, 1535–1549. (doi:10.1175/1520-0442(2001)014<1535:GIVISS>2.0.CO;2)
15. James R, Washington R, Rowell DP. 2013 Implications of global warming for the climate of African rainforests. *Phil. Trans. R. Soc. B* **368**, 20120298. (doi:10.1098/rstb.2012.0298)
16. Malhi Y, Adu-Bredu S, Asare RA, Lewis SL, Mayaux P. 2013 African rainforests: past, present and future. *Phil. Trans. R. Soc. B* **368**, 20120312. (doi:10.1098/rstb.2012.0312)

17. Hernandez M, Ummenhofer CC, Anchukaitis KJ. 2015 Multi-scale drought and ocean–atmosphere variability in monsoon Asia. *Environ. Res. Lett.* **10**, 074010. (doi:10.1088/1748-9326/10/7/074010)
18. L'Heureux ML *et al.* 2017 Observing and predicting the 2015/16 El Niño. *Bull. Amer. Meteor. Soc.* **98**, 1363–1382. (doi:10.1175/BAMS-D-16-0009.1)
19. Jiménez-Muñoz JC, Mattar C, Barichivich J, Santamaría-Artigas A, Takahashi K, Malhi Y, Sobrino JA, van der Schrier G. 2016 Record-breaking warming and extreme drought in the Amazon rainforest during the course of El Niño 2015–2016. *Sci. Rep.* **6**, 33130. (doi:10.1038/srep33130)
20. Betts RA, Jones CD, Knight JR, Keeling RF, Kennedy JJ. 2016 El Niño and a record CO_2 rise. *Nat. Clim. Change* **6**, 806–810. (doi:10.1038/nclimate3063)
21. Yue C, Ciais P, Bastos A, Chevallier F, Yin Y, Rödenbeck C, Park T. 2017 Vegetation greenness and land carbon-flux anomalies associated with climate variations: a focus on the year 2015. *Atmos. Chem. Phys.* **17**, 13 903–13 919. (doi:10.5194/acp-17-13903-2017)
22. Liu J *et al.* 2017 Contrasting carbon cycle responses of the tropical continents to the 2015–2016 El Niño. *Science* **358**, 191. (doi:10.1126/science.aam5690)
23. Dee DP *et al.* 2011 The ERA-Interim reanalysis: configuration and performance of the data assimilation system. *Q. J. R. Meteorol. Soc.* **137**, 553–597. (doi:10.1002/qj.828)
24. Simmons AJ, Berrisford P, Dee DP, Hersbach H, Hirahara S, Thépaut JN. 2017 A reassessment of temperature variations and trends from global reanalyses and monthly surface climatological datasets. *Q. J. R. Meteorol. Soc.* **143**, 101–119. (doi:10.1002/qj.2949)
25. Wells N, Goddard S, Hayes MJ. 2004 A self-calibrating palmer drought severity index. *J. Clim.* **17**, 2335–2351. (doi:10.1175/1520-0442(2004)017<2335:ASPDSI>2.0.CO;2)
26. van der Schrier G, Barichivich J, Briffa KR, Jones PD. 2013 A scPDSI-based global data set of dry and wet spells for 1901–2009. *J. Geophys. Res. Atmos.* **118**, 4025–4048. (doi:10.1002/jgrd.50355)
27. Trenberth KE, Dai A, van der Schrier G, Jones PD, Barichivich J, Briffa KR, Sheffield J. 2014 Global warming and changes in drought. *Nat. Clim. Change* **4**, 17–22. (doi:10.1038/nclimate2067)
28. Beck HE, Van Dijk AIJM, Levizzani V, Schellekens J, Miralles DG, Martens B, De Roo A. 2017 MSWEP: 3-hourly 0.25° global gridded precipitation (1979–2015) by merging gauge, satellite, and reanalysis data. *Hydrol. Earth Syst. Sci.* **21**, 589–615. (doi:10.5194/hess-21-589-2017)
29. Food and Agriculture Organization. 2003 Digital soil map of the world and derived soil properties: cd-rom. Rome, Italy: FAO.
30. Takahashi K, Montecinos A, Goubanova K, Dewitte B. 2011 ENSO regimes: reinterpreting the canonical and Modoki El Niño. *Geophys. Res. Lett.* **38**, L10704. (doi:10.1029/2011GL047364)
31. Clarke AJ, Kim KY. 2005 On weak zonally symmetric ENSO atmospheric heating and the strong zonally symmetric ENSO air temperature response. *J. Atmos. Sci.* **62**, 2012–2022. (doi:10.1175/JAS3448.1)
32. Alexander MA, Bladé I, Newman M, Lanzante JR, Lau NC, Scott JD. 2002 The atmospheric bridge: the influence of ENSO teleconnections on air–sea interaction over the global oceans. *J. Climate* **15**, 2205–2231. (doi:10.1175/1520-0442(2002)015<2205:TABTIO>2.0.CO;2)
33. Sulca J, Takahashi K, Espinoza JC, Vuille M, Lavado-Casimiro W. 2017 Impacts of different ENSO flavors and tropical Pacific convection variability (ITCZ, SPCZ) on austral summer rainfall in South America, with a focus on Peru. *Int. J. Climatol.* **38**, 420–435. (doi:10.1002/joc.5185)
34. Ropelewski CF, Halpert MS. 1987 Global and regional scale precipitation patterns associated with the El Niño/Southern Oscillation. *Mon. Weather Rev.* **115**, 1606–1626. (doi:10.1175/1520-0493(1987)115<1606:GARSPP>2.0.CO;2)
35. Schollaen K, Karamperidou C, Krusic P, Cook E, Helle G. 2015 ENSO flavors in a tree-ring $\delta^{18}O$ record of *Tectona grandis* from Indonesia. *Clim. Past* **11**, 1325–1333. (doi:10.5194/cp-11-1325-2015)
36. Takahashi K, Dewitte B. 2016 Strong and moderate nonlinear El Niño regimes. *Clim. Dyn.* **46**, 1627–1645. (doi:10.1007/s00382-015-2665-3)
37. Takahashi K, Martínez AG. 2017 The very strong coastal El Niño in 1925 in the far-eastern Pacific. *Clim. Dyn.* (doi:10.1007/s00382-017-3702-1)
38. Erfanian A, Wang G, Fomenko L. 2017 Unprecendented drought over tropical South America in 2016: significantly under-predicted by tropical SST. *Sci. Rep.* **7**, 5811. (doi:10.1038/s41598-017-05373-2)
39. Panisset JS, Libonati R, Gouveia CMP, Machado-Silva F, França DA, França JRA, Peres LF. 2017 Contrasting patterns of the extreme drought episodes in 2005, 2010 and 2015 in the Amazon Basin. *Int. J. Climatol.* **38**, 1096–1104. (doi:10.1002/joc.5224)
40. Lima CHR, AghaKouchak A. 2017 Droughts in Amazonia: spatiotemporal variability, teleconnections, and seasonal predictions. *Water Resour. Res.* **53**, 10 824–10 840. (doi:10.1002/2016WR020086)
41. Zou Y, Macau EEN, Sampaio G, Ramos, AMT, Kurths J. 2016 Do the recent severe droughts in the Amazonia have the same period of length? *Clim. Dyn.* **46**, 3279–3285. (doi:10.1007/s00382-015-2768-x)
42. Andreoli RV, Soares de Oliveira S,Kayano MT, Viegas J, Ferreira de Souza RA, Candido LA. 2017 The influence of different El Niño types on South American rainfall. *Int. J. Climatol.* **37**, 1374–1390. (doi:10.1002/joc.4783)
43. Bowman KW *et al.* 2017 Global and Brazilian carbon response to El Niño Modoki 2011–2010. *Earth Space Sci.* **4**, 637–660. (doi:10.1002/2016EA000204)
44. Asefi-Najafabady S, Saatchi S. 2013 Response of African humid tropical forests to recent rainfall anomalies. *Phil. Trans. R. Soc. B* **368**, 20120306. (doi:10.1098/rstb.2012.0306)
45. Malhi Y, Wright J. 2004 Spatial patterns and recent trends in the climate of tropical rainforest regions. *Phil. Trans. R. Soc. Lond. B* **359**, 311–329. (doi:10.1098/rstb.2003.1433)
46. Taufik M, Torfs PJJF, Uijlenhoet R, Jones PD, Murdiyarso D, Van Lanen HAJ. 2017 Amplification of wildfire area burnt by hydrological drought in the humid tropics. *Nat. Clim. Change* **7**, 428–431. (doi:10.1038/nclimate3280)
47. Di Giuseppe F, Molteni F, Dutra E. 2013 Real-time correction of ERA-Interim monthly rainfall. *Geophys. Res. Lett.* **40**, 3750–3755. (doi:10.1002/grl.50670)